# Harmonics Characteristic Of Electromotive Force And Thermal Analysis In Superconducting Synchronous Generator

Young-Sik Jo, Jung-Pyo Hong, Gyu-Tak Kim, Youg-Kil Kwon*, Kang-Sik Ryu*
Dept. of Electrical Engineering, ChangWon Nat'l Univ.
9 Sarim-dong, Chang-won, Kyong-nam, 641-773, Korea.
Korea Electrotechology Reserch Institute*
28-1 Sungju-dong, Chang-won, Kyong-nam, 641-120, Korea.*.

## Abstract

A 30 kVA calss superconducting synchronous generator has been analyzed. Magnetic field distribution has been calculated by 3D finite element method(FEM) and analytical method at no-load condition. And we studied the thermal distribution using FEM at rated load. Electromotive force(EMF) of armature coil is varied to the field coil distribution, we examined the EMF including harmonic analysis.

## 1. Introduction

In this paper, 30kVA class superconducting synchronous generator(SSG) was studied. Since the field winding is the superconducting part of the machine, it must be kept cold and so is carried on an insulating structure and fed with cryogenic coolant. A SSG have different structure so air-gap length became larger than general generator.
The flux distribution varies with according to z-direction because of field coil winds on air bobbin and have large air-gap length.
Thus 2D analysis can't give information of the field distribution considering z-direction so 3D analysis is required. This paper compared the 2D results with 3D ones of electricmotive force according to field coil width and presented temperature distribution at rated-load in stator using by 2D FEM.

## 2. Machine Layout

A radiation shield is required to intercept infrared radiation from the ambient temperature parts of the machine. This shield has a temperature that is intermediate between that of the field winding and ambient. The thermal radiation shield also serves as a shield for time-varying magnetic flux. Flux shielding is required because AC fields would producing dissipation in the cold space. The stator have air-duct to reduce increasing temperature in stator.

Machine layout is showen in Fig. 1.

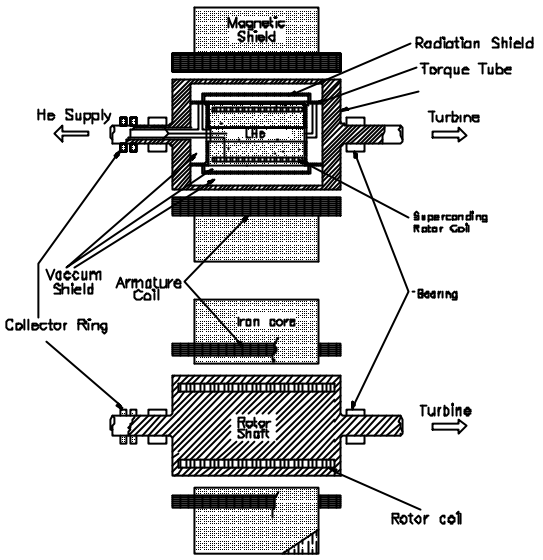


Fig. 1 SSG : side view cross section

## 3. Electromagnetic field analysis

### 3.1 Analysis model

SSG is simply modeled in 3D because it consist of nonmagnetic material except magnetic shield.

Table 1. brief specifications

| power | pole | rate speed | freq. | field type |
|---|---|---|---|---|
| 30kVA | 4 | 1800[rpm] | 60[Hz] | Racetrack |

Analysis model is shown in Fig. 2. Governing equation is given as equation (1) by using field variable with magnetic scalar potential.[1][3]

$$\nabla \cdot (\mu \nabla \Omega) = \nabla \cdot \mu \boldsymbol{H}_c \qquad (1)$$
$$\nabla \times \boldsymbol{H}_c = \boldsymbol{J}_c$$

Where $\mu$ is the permeability in shield, $\Omega$ is the magnetic scalar potential.

Applying the Galerkin method to the governing equation, the following system equation is derived.

$$[S][\Omega] - [F] = 0 \qquad (2)$$

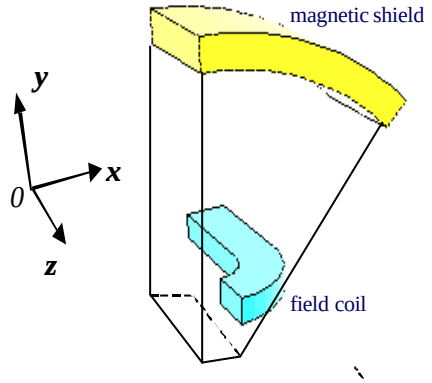


Fig. 2 analysis model

Analysis model was classified three type according to field coil width as shown in Table 2.

Table 2 classification of model unit: [mm]

| | case 1 | case 2 | case 3 |
|---|---|---|---|
| field coil width | 21.85 | 26.85 | 31.85 |

In 2D analysis, we applied the Biot-Savart's law and image method.[2]

$$dH = \frac{Id\boldsymbol{L} \times \boldsymbol{R}}{4\pi |\boldsymbol{R}|^3} \qquad (3)$$

### 3.2 Analysis result

In radial component of flux density, the 2D analysis results was higher than 3D numerical results in all case. Fig. 3 shows the analysis results, the difference between 2D and 3D was 0.03 [T] in case 1, 0.02[T] in case 2 and 0.01[T] in case 3.

For an optimal use of the superconductor and save operation of the superconducting coil an exact knowledge of the magnetic field and temperature distribution within the superconductor is necessary. Fig 4 represent magnetic field distribution at middle plan of superconducting field coil (y=85.63[mm]). In case 2, axial length of magnetic shield is 96[mm], field coil turns is 531 and exciting current is 200[A]. Maximum magnitude of $B$ was 2.14[T] and placed at starting point of return path.

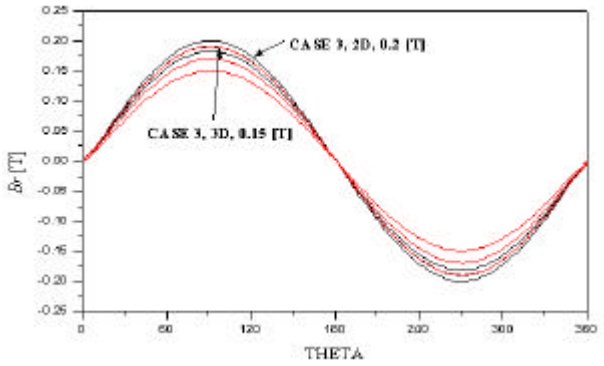


Fig. 3 distribution of $B_r$ at armature coil (z=0)

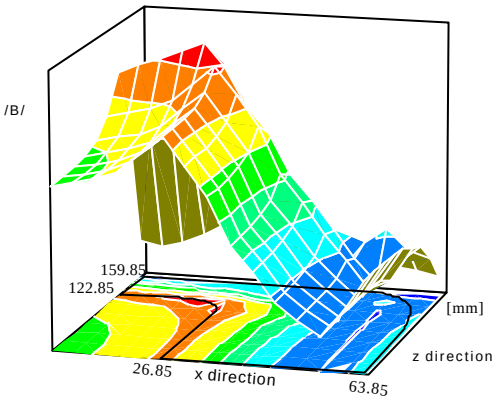


Fig 4 distribution of $/B/$ at x-z plan (y=85.63)

Fig. 5 and 6 shown distribution of $B_r$ of the case 1 and case 3 at z=96[mm]. Comparing case 1 with case 3, the $B_r$ of the case 3 was higher than case 1. It will directly affect to the electromotive force.

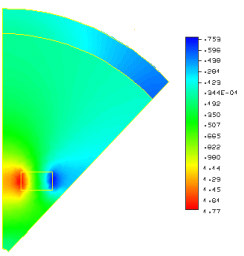

Fig 5 distribution of $B_r$(case 1)

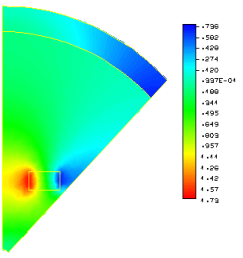

Fig. 6 distribution of $B_r$ (case 3)

### 3.3 Electromotive Force

Armature coil was Y connection, double layer winding, 7/9 short pitch, 3 slots per pole per phase. The 2D results were higher than 3D results by 50% in case 1, 37% in case 2 and 27% in case 3.

Radial flux density distribution is shown in Fig. 7.

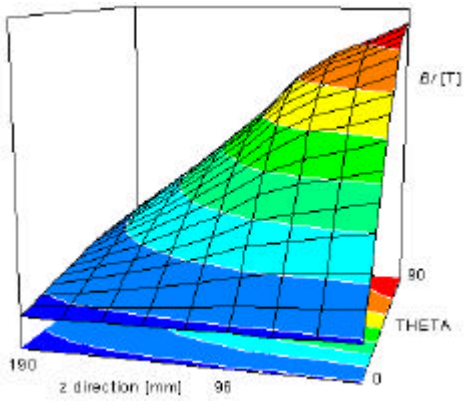


Fig. 7 distribution of $B_r$

Induced voltage of the armature coil is shown Fig. 8.

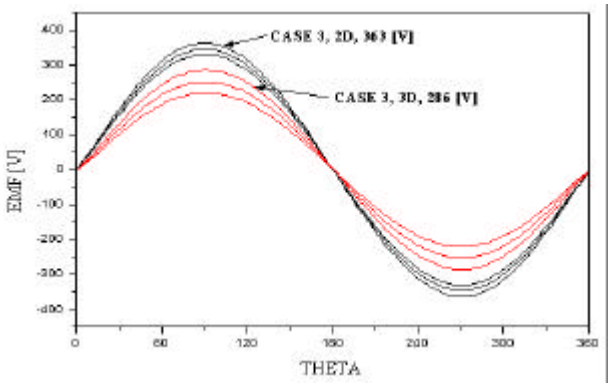


Fig. 8 electromotive force

If armature winding transfer full pitch, we will expect higher EMF. Slot harmonics are ignored because long air-gap length and armature structure made by fiber reinforced plastics(FRP). The Case which changed to full pitch armature winding is shown in Fig. 9.

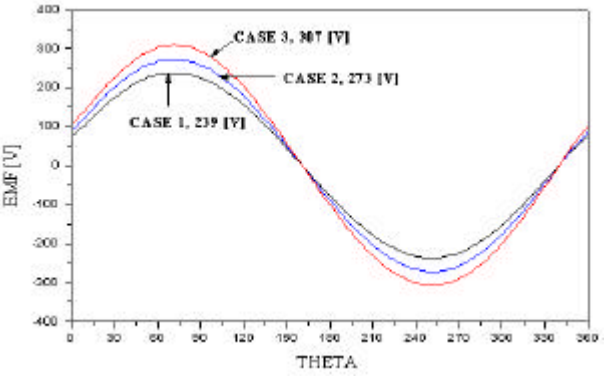


Fig. 9 EMF (full Pitch)

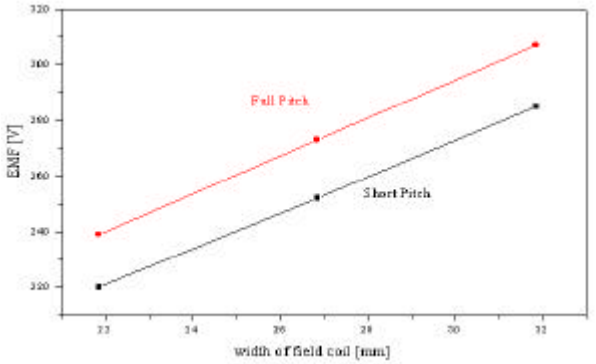


Fig. 10 EMF according to width of field coil

EMF increased 20[V] in case 1, case 2 and increased 30[V] in case 3.

Harmonic distortion factor of the EMF was examined. It was calculated up to 100th order. The results are shown in Table 3.

Table 3 distortion factor unit: %

| | case 1 | case 2 | case 3 |
|---|---|---|---|
| short pitch | 0.47 | 0.30 | 0.31 |
| full pitch | 0.94 | 0.52 | 0.47 |

## 4. Thermal Analysis

For thermal analysis of armature, we assume that heat generated per unit volume per slot is equally distributed in slots and same value at rated load. Thus we applied the periodic boundary condition on both side.

2D governing equation is (4). If thermal conductivity is to be isotropic inner space, it becomes constant.

$$k\left(\frac{\partial T}{\partial x^2} + \frac{\partial^2 T}{\partial y^2}\right) + \overline{q} = 0 \qquad (4)$$

Element matrix [k] and heat-transfer rate vector {f} as follow.

$$[k^{(e)}] = \int_{\Omega^e} k\left(\frac{\partial [N]^T}{\partial x}\frac{\partial [N]}{\partial x} + \frac{\partial [N]^T}{\partial y} + \frac{\partial [N]}{\partial y}\right) d\Omega + \int_{s_1^e} h_c [N]^T [N] ds + \int_{s_1^e} h_r [N]^T [N] ds$$

$$\{f^{(e)}\} = \int_{\Omega^e} Q[T]^T d\Omega - \int_{\pi^e} \overline{q}\,[N]^T ds + \int_{s_1^e} h_c T_c [N]^T ds + \int_{\pi_1^e} h_r T_r [N]^T ds$$

Condition of thermal analyze for armature represent in Table 4.

Table 4 parameters for thermal analysis

| | |
|---|---|
| $h_{out}$ | 16 [W/m$^2$ °C ] |
| $k_{Al}$ | 204 [W/m °C ] |
| $k_{mag}$ | 43 [W/m °C ] |
| $k_f$ | 0.5 [W/m °C] |
| $k_c$ | 386 [W/m °C] |
| $h_{gap}$ | 40 [W/m$^2$ °C] |

Where $h_{out}$ is out of frame convection coff., $k_{Al}$ is thermal conductivity at frame, $k_{mag}$ is thermal conductivity at magnetic shield, $k_f$ is thermal conductivity at armature, $k_c$ is thermal conductivity at coil, $h_{gap}$ is convection coff. at air-gap.

The generator have a cooling fan and generated heat per unit volume was calculated 85,594[W/m$^3$]. In the results, maximum temperature is 62.5[℃] and minimum temperature is 47.2[℃]. Temperature distribution shown in Fig.11.

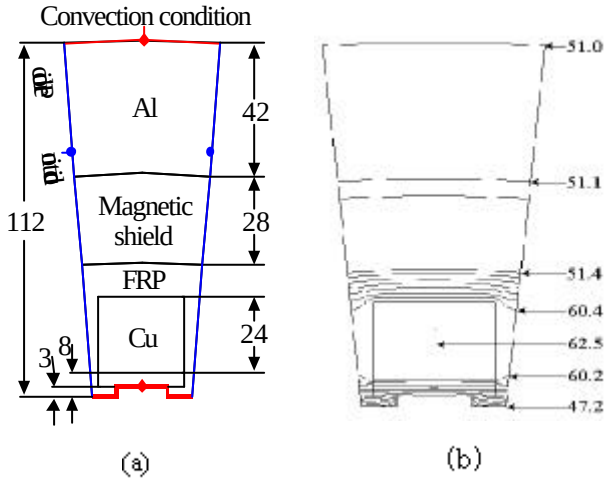


Fig.11 analysis model and equi-thermal line

## 5. Conclusion

In this paper, we studied the EMF and thermal distribution of A 30 kVA calss superconducting synchronous generator. Magnetic field distribution has been calculated by 3D finite element method and 2D analytical method at no-load condition. The thermal distribution was analyzed using FEM at rated load. EMF characteristic of armature coil was performed when the field coil distribution is varied and harmonic analysis was carried out.

## 6. reference


[1] S.J.SALON, "Finite Element analysis of electrical machines", 125~135,1995

[2] Hague , "The Principles of Electromagnetism", 104-114, 1995

[3] J.N.Reddy, "An Introduction to the Finite Element method", 408,1984

[4] J.P.Holman,"Heat Transfer", 349, 1992